Assignment of 4*f*-5*d* absorption bands in Ce-doped $R\mathrm{AlO_3}$ (R=La, Gd, Y, Lu) perovskites

E. Mihóková,[1,2] M. Nikl,[1] M. Bacci,[3] M. Dušek,[1] and V. Petříček[1]
[1]*Institute of Physics, Academy of Sciences of the Czech Republic, Cukrovarnická 10, 16253 Prague 6, Czech Republic*
[2]*Department of Materials Science, University of Milano-Bicocca, Via Cozzi 53, 20125 Milan, Italy*
[3]*Institute of Applied Physics "N. Carrara," CNR, Via Madonna del Piano 10, 50019 Sesto Fiorentino, Italy*
(Received 20 February 2009; revised manuscript received 22 April 2009; published 28 May 2009)

An intuitive assignment of absorption bands of Ce-doped $R\mathrm{AlO_3}$ (R=Gd, Y, and Lu) perovskites suggested by some authors is compromised. We use semiempirical approaches based on the extended Hückel method to calculate the energy-level scheme of the cluster containing Ce and its nearest O neighbors in true $R\mathrm{AlO_3}$ (R=La, Gd, Y, and Lu) structures. Our calculations show a different origin for the energy levels involved in the absorption process than might intuitively be suggested. Some quantitative aspects also reasonably correspond to experimental observation.

DOI: 10.1103/PhysRevB.79.195130 PACS number(s): 42.70.−a, 78.20.Bh, 78.40.−q

I. INTRODUCTION

The Ce^{3+} ion was doped in the yttrium aluminum garnet (YAG) single crystal and characterized by electron paramagnetic resonance methods already in the mid-60s of the last century[1] when this crystal had been grown by the innovative Czochralski technique as one of the first oxide systems.[2] 5*d*-4*f* luminescence of Ce^{3+} in YAG was reported in 1973 (Ref. 3) and some years later the potential of this system for electron detection in scanning electron microscopy, i.e., its application as fast scintillator, was noted.[4] At the beginning of the 1970s another stoichiometric composition between Y_2O_3 and Al_2O_3, namely, the perovskite $YAlO_3$, was prepared in the form of a single crystal, both undoped as well as Ce^{3+} doped.[5] The latter was found even more promising for fast scintillator applications.[6,7] To increase the density and effective atomic number of the $YAlO_3$:Ce scintillator, several laboratories around the world were involved in intense research work in the 90s of the last century to replace the yttrium cation fully or partially by the lutetium ion; for a review see Ref. 8.

The detailed description of splitting of the Ce^{3+}-excited 5*d* and ground 4*f* states due to both the site symmetry and crystalline field was reported already in 1971 in $MePO_4$ structure (Me=Sc, Y, and Lu).[9] Somewhat later, similar considerations in the YAG host were published[10] and recently reviewed and reconsidered.[11] Due to tetragonal symmetry of the dodecahedral yttrium site in YAG, the 5*d* state splits into lower-lying doublet ^2E_g and upper-lying triplet $^2T_{2g}$ level which are further split due to given symmetry and spin-orbit interaction into five levels giving rise to five well-known absorption bands at 458 and 340 nm (transitions to split levels originated from ^2E_g) and 261, 224, and 205 nm (transitions to split levels originated from $^2T_{2g}$).[12] To our knowledge, such detailed assignment of Ce^{3+} 5*d*-level splitting in YAP host has never been done. Absorption spectra of YAP:Ce showing a set of three closely lying bands at 303, 291, and 275 nm and additional pair of bands at 237 and 219 nm, may intuitively suggest an inverted order of ^2E_g and $^2T_{2g}$ levels.[5,13] In addition, absorption spectra of Ce^{3+}-doped $GdAlO_3$ and $LuAlO_3$ are qualitatively very similar.[8,12,14] A hypothesis of inverted-level order (^2E_g versus $^2T_{2g}$) could be further motivated by the consideration that unlike in the ideal perovskite structure, the closest neighborhood of *R* ion in the real structure is composed by only six oxygens. Such coordination would then result in an octahedral-like symmetry of yttrium site in YAP.[15] Symmetry considerations are indeed complicated by the distortion of the ideal perovskite lattice, a cubo-octahedral coordination of *R* ion, which increases with decreasing size of the *R* cation.[12] In fact, in the calculation of the splitting of the 4*f* ground-state levels in YAP host[16] the leading term in the Hamiltonian of the system is that of cubic symmetry. Distortion of perovskite lattices of ABX_3 formula was also the subject of recent studies due to both the high number and practical importance of materials in this group.[17,18]

Due to the unclear origin of the observed absorption bands related to 4*f*-5*d* transitions of Ce^{3+} ion in aluminum perovskite lattices and somewhat conflicting views in the literature in this respect we calculate the splitting of 5*d* orbitals of Ce^{3+} ion in several real perovskite structures $R\mathrm{AlO_3}$ (R=La, Gd, Y, and Lu). The results provide an excellent qualitative explanation of the pattern observed in absorption spectra as well as reasonable quantitative agreement of experimental and calculated data.

II. EXPERIMENTAL DETAILS

The absorption spectra were measured by the Spectrophotometer Shimadzu K3101PC using 0.5–1-mm-thick polished plates of single crystals of Ce-doped $YAlO_3$ and $LuAlO_3$. The former was grown by micropulling-down in IMRAM, Tohoku University, Sendai (see Ref. 19) while the latter by Czochralski technique in the Institute of Electronic Materials Technology, Warsaw (see Ref. 20).

III. RESULTS AND DISCUSSION

Absorption spectra of Ce^{3+} in $YAlO_3$ (YAP) and $LuAlO_3$ (LuAP) hosts are displayed in Fig. 1. There are five absorption bands in the spectrum corresponding to electronic transitions to excited energy levels derived from 5*d* orbitals of Ce^{3+} ion. There is a group of three low-energy absorption bands followed by a *gap* and a higher pair of two absorption

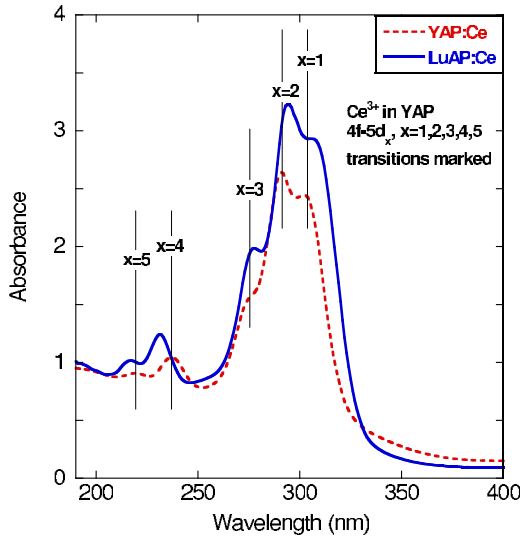

FIG. 1. (Color online) RT-absorption spectra of Ce^{3+} in YAP and LuAP hosts.

bands. The gap observed in LuAP:Ce is larger with respect to that of YAP:Ce. As mentioned above, the observed absorption scheme "3+2" may lead to a temptation to assign absorption bands intuitively to electronic transitions to the 5*d* orbitals of Ce^{3+} fundamentally split by octahedral field, namely, lower-lying triplet T_{2g} and upper-lying doublet E_g, further split by additional field of lower symmetry. In greater detail such picture presumes that the Ce^{3+} ion is in ideal case embedded in an octahedral field of nearest-neighboring oxygens. However, the real perovskite structure is slightly distorted with respect to the ideal one. Such distortion then leads to a splitting of T_{2g} and E_g levels resulting in the corresponding 3+2 absorption spectrum. Below we show that as much as an intuitive assignment just described might look reasonable it does not reflect the actual situation.

A. Rare-earth-ion perovskite structure

The rare-earth ion in perovskites is surrounded by 12 oxygen ions forming cuboctahedral coordination.[12] Along the sequence La, Gd, Y to Lu, the rare-earth ion becomes too small for 12-fold coordination and the perovskite phase will be distorted.[12] The new polyhedra are defined as distorted bicapped prisms. In Ref. 21 the authors claim that these bicapped prisms can be related to the cuboctahedral ones by the loss from the latter of four oxygen ions (coordination 8) located on four opposite edges in the unit cell (purple oxygens number 9, 10, 11, and 12 in Fig. 2). However, as it turns out, this picture is not fully accurate. To obtain a more precise idea how various perovskite structures are related to those cuboctahedral, we compared 12-coordinated *R*-O complex in the real structure of aluminum perovskites with that of cuboctahedral arrangement (see Fig. 3). The crystallographic data in Table I clearly demonstrate the structural diversity of the real perovskites where atoms in $LaAlO_3$ are almost completely fixed by the symmetry while the others have most of the parameters free. What can be seen in Fig. 3 was constructed in the following way. The atomic coordi-

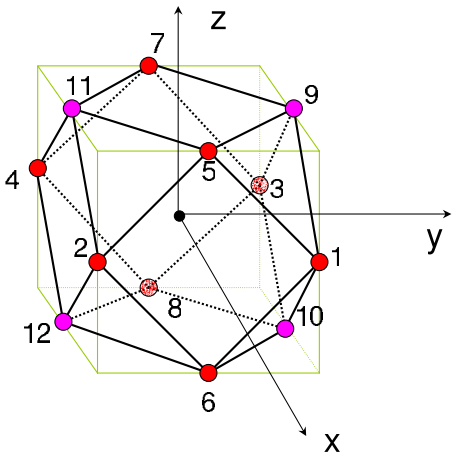

FIG. 2. (Color online) Cuboctahedron corresponding to an ideal 12-coordinated *R*-O complex. *R* is in the middle; numbered spheres are oxygens. The distances change according to the *R* ion. The *R*-O distance in such ideal case would be 2.68 Å in $LaAlO_3$, 2.64 Å in $GdAlO_3$, 2.62 Å in $YAlO_3$, and 2.60 Å in $LuAlO_3$. The numbers are obtained by optimization procedure described in the text.

nates of the ideal and real perovskite structure (excluding aluminum) were transformed to a common coordinate system. Then the coordinates of both structures were translated

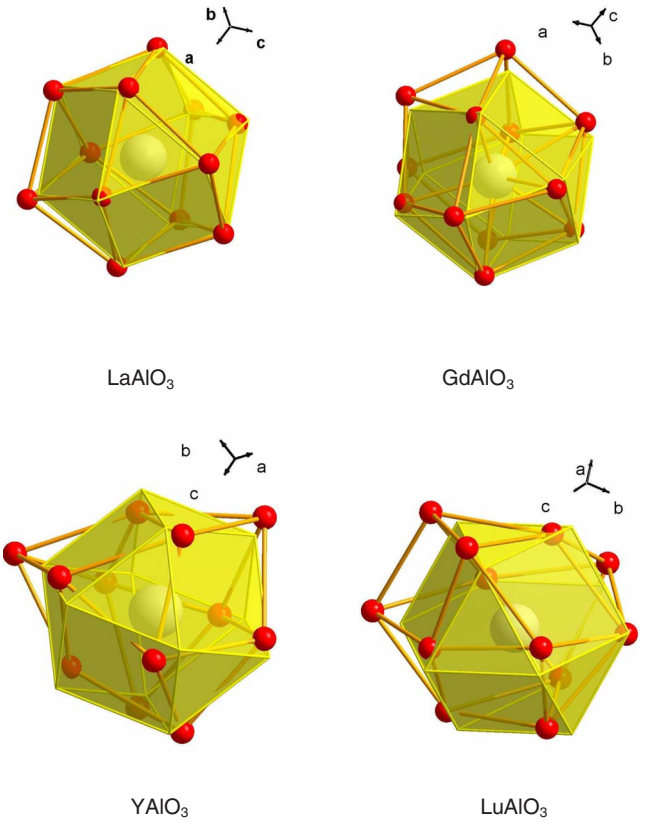

FIG. 3. (Color online) 12-coordinated *R*-O complex in the real structure of $RAlO_3$. *R* is the large white sphere in the middle; O are the small red spheres around. The yellow unit is an ideal cuboctahedron to which the real structure is compared. In the sequence La, Gd, Y, and Lu one can notice progressive deformation of the complex with respect to the ideal cuboctahedron.

TABLE I. Crystallographic data of $REAlO_3$ (RE=La, Gd, Y, and Lu).

	a	b	c	Symmetry	R^a	ICSD[b]
RE	Fractional coordinates of *RE* and O					
La (Ref. 31)	5.3653(2)	5.3653(2)	13.112(1)	*R*-3*c*	0.0590	92522
	La [0,0,0.25]					
	O [0.448(2) 0 0.25]					
Gd (Ref. 32)	5.3049(7)	7.4485(9)	5.2537(6)	*Pnma*	0.0117	59848
	Gd [0.462223(7), 0.25, −0.008091(7)]					
	O1[0.01389(12), 0.25, 0.07210(12)]; O2[0.28504(8), −0.03823(6), 0.21534(8)]					
Y (Ref. 33)	5.32951(16)	7.37059(12)	5.18027(38)	*Pnma*	0.0180	99419
	Y [0.44695(7), 0.25, −0.01192(7)]					
	O1[0.0225(5), 0.25, 0.0840(6)]; O2[0.2949(3), −0.0441(2),0.2049(3)]					
Lu[c]	5.3315(3)	7.3030(4)	5.1041(3)	*Pnma*	0.0271	
	Lu [0.43762(6), 0.25, −0.01524(8)]					
	O1[0.0287(10), 0.25, 0.0962(14)], O2[0.2989(6), −0.0498(4), 0.1985(8)]					

[a]$\Sigma| |F_o|-|F_c| | / \Sigma |F_o|$, where F_o and F_c are observed and calculated structure factors.
[b]Code in the Inorganic Crystal Structure Database maintained by the National Institute of Standards and Technology (NIST) and Fachinformationszentrum Karlsruhe (FIZ), Germany.
[c]Current work, the details will be described elsewhere.

to get the central R atoms at the origin. Finally the real structure was rotated around three independent axes and the ideal structure was scaled (i.e., shrunk or expanded) until we reached—using standard least-squares procedure—the minimal sum of distances between the ideal and real oxygen positions. For this calculation we modified the standard crystallographic rigid body procedure in the computing system JANA2006, which is normally used for refinement of crystal structures with well-defined rigid objects.

The above described comparison demonstrates that four oxygens in maximum distance from R correspond to oxygens lying on opposite edges of two neighboring sides of the reference cubic cell (e.g., numbers 1, 2, 11, and 12 in Fig. 2). An exception is $LaAlO_3$ that remains more symmetric (D_3 symmetry) and derives from cuboctahedron in such a way that six oxygens forming an octahedron stay in place while the distance of three (1, 7, and 12 of Fig. 2) equally shrinks and the distance of other three (4, 6, and 9 of Fig. 2) equally elongates.

B. Energy-level scheme of Ce-O complex

To calculate the energy-level scheme of the Ce-O complex, involving Ce ion with 12 nearest oxygen neighbors corresponding to the true perovskite structures, we used two approaches. Both of them are based on Wolfsberg and Helmholtz[22] approximation. The first is an angular overlap method (AOM) (see, e.g., Refs. 23–25) and the second is program CACAO (Computer Aided Composition of Atomic Orbitals)[26] using the extended Hückel method.[27]

AOM is one-center treatment, neglecting the contributions arising from interactions among ligands; therefore, only semiquantitative results can be obtained when the strong covalent effects occur. AOM should give underestimated but still qualitatively correct results. The energy change e_λ of a given R orbital, due to the interaction with a ligand (oxygen) orbital, is given by

$$e_\lambda = K_\lambda S_\lambda^2 F_{\lambda\omega}^2, \tag{1}$$

where λ indicates the bonding symmetry with respect to the R-oxygen axis ($\sigma, \pi, \ldots$) and ω specifies the particular orbital; S_λ is the diatomic overlap integral and $F_{\lambda\omega}$ is a fraction of the maximum overlap integral and depends on the angular coordinates of the ligands; K_λ is the proportionality constant. For not-too-large variations in metal-ligand distance in Refs. 24 and 25, it was found that energies e_λ can be satisfactorily fit by an exponential law of the type

$$e_\lambda = a_\lambda \exp(-b_\lambda R). \tag{2}$$

Moreover, as numerous previous calculations showed, the contribution of energy e_π is considerably smaller than that of e_σ, namely, about 20% of the e_σ value.

We applied the above approximation for e_π and expression (2) to energies e_σ with a_σ=1 and b_σ from the interval [Eqs. (1) and (2)]. (Note, that the value a_σ does not change the relative separations of energy levels and, therefore, the qualitative frame of resulting energy scheme.) Under these assumptions we obtained the following. In the case of ideal cuboctahedral environment the energy-level scheme is composed by the low-lying E_g doublet (formed by d orbitals z^2 and x^2-y^2) and above-lying T_{2g} triplet (formed by d orbitals xy, xz, and yz). Therefore the splitting of d orbitals is the same as in the case of cubic field (unlike octahedral field).

In the case of $LaAlO_3$ (LaAP) with the smallest lattice deformation and the 12-coordinated R arrangement closest to the ideal cuboctahedron (cf. Fig. 3) the energy-level scheme is also close to the one of ideal cuboctahedron. The lowest level is double-degenerate E_g (formed by d orbitals z^2 and x^2-y^2) with above-lying former triplet T_{2g} split in a singlet and doublet in accordance with what is reported in Refs. 12,

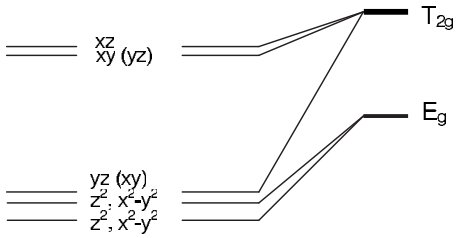

FIG. 4. Splitting of 5*d* orbitals of Ce^{3+} ion in the nearest-neighboring oxygen field in $RAlO_3$ (R=Gd, Y, and Lu) given by AOM for $b_\sigma < 3$ (see the text). For R=Lu there is a switch in position of *yz* and *xy* orbitals (corresponding orbital for R=Lu is given in parenthesis). Different *d* orbitals are for simplicity referred to as, e.g., *xy* instead of d_{xy}, etc.

28, and 29. The triplet splitting is rather small. All three orbitals are predominantly a mixture of *d* orbitals *xy*, *xz*, and *yz*. For all other structures $RAlO_3$ (R=Gd,Y, and Lu) the energy scheme corresponds to the scheme seen in absorption spectra (Fig. 1). In other words there are three low-lying singlet levels and after a certain gap there are two upper singlet levels. However, this energy scheme is not derived from the lower-split triplet T_{2g} and upper-split doublet E_g, as intuitively suggested. Rather than that, two of the lowest three levels are mostly composed of split E_g doublet while one of them is predominantly one level of the T_{2g} triplet. Its separation from former E_g levels becomes smaller with respect to that of higher levels of split triplet. There is also significant mixing between E_g and T_{2g} levels. The scheme with predominant composition of levels is displayed in Fig. 4.

As the value of b_σ reaches the value 3 and higher, there is higher mixing and in the case of YAP even a level crossing as schematically shown in Fig. 5. However, the principal arrangement of energy levels stays the same. Or in other words there are three lower levels two of which though are predominantly composed by former doublet E_g. To summa-

TABLE II. Excited-state energies and molecular-orbital populations of 12-coordinated Ce-O complex in various perovskite crystal structures calculated by CACAO. Different *d* orbitals are, for simplicity, referred to as, e.g., *xy* instead of d_{xy}, etc.

Crystal structure	E (eV)	x^2-y^2 (%)	z^2 (%)	*xy* (%)	*xz* (%)	*yz* (%)
Cuboctahedron	−6.180	22	74			
	−6.180	74	22			
	−5.977			95		
	−5.977				5	90
	−5.977				90	5
LaAP	−6.133	67	22	2	2	6
	−6.133	22	67	5	5	
	−5.860	7	2	15	15	59
	−5.860	2	7	44	44	
	−5.821			33	33	33
GdAP	−6.084	63	8	27		
	−5.961	2	87	9		
	−5.923				2	97
	−5.358	33	3	60		
	−5.204				95	2
YAP	−6.096	56	2	39		
	−5.806				3	95
	−5.798		94	3		
	−4.905	41		53		
	−4.892				93	3
LuAP	−6.081	7	45		45	
	−5.680	73	23		2	
	−5.666			92		6
	−4.669			6		90
	−4.410	16	30		48	

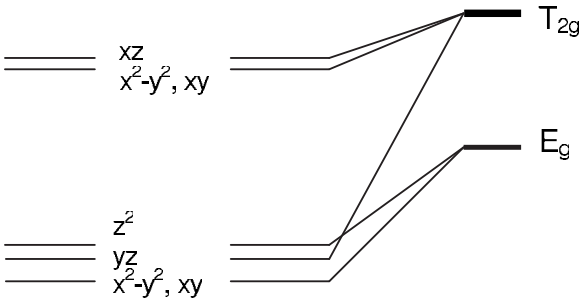

FIG. 5. Splitting of 5*d* orbitals of Ce^{3+} ion in the nearest-neighboring oxygen field in $RAlO_3$ (R=Gd, Y, and Lu) given by AOM for $b_\sigma > 3$ (see the text). Different *d* orbitals are for simplicity referred to as, e.g., *xy* instead of d_{xy}, etc.

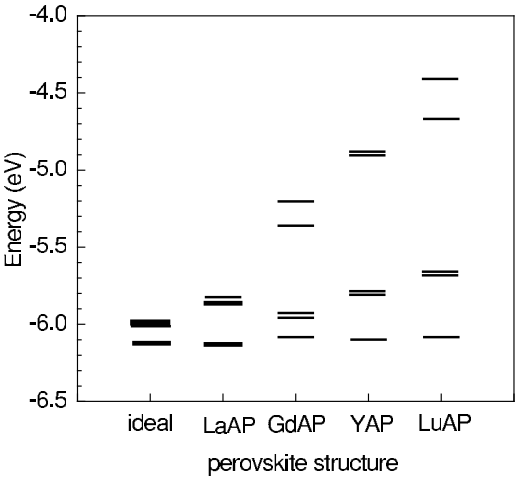

FIG. 6. Excited-state energies of 12-coordinated Ce-O complex in various perovskite crystal structures calculated by CACAO (numerical values as reported in Table II).

rize, for substantially wide range of parameter b_σ the AOM calculation provides energy-level scheme compatible with experimental data, although showing a level composition different from what was intuitively suggested.

Since the AOM calculation involves approximation (2) to refine the results we also used another approach based on extended Hückel method and the program CACAO as mentioned above. The program uses a database of parametrized input for each atom of the cluster. The scheme of energy levels obtained by CACAO qualitatively corresponds to that obtained by AOM described in the text and for GdAP, YAP, and LuAP, schematically shown in Figs. 4 and 5. The energy values and compositions of orbitals are listed in Table II and corresponding energy schemes of all discussed perovskite structures are displayed in Fig. 6. One can see that the gap between the lower three and upper two levels increases as the structure becomes more deformed (in the sequence GdAP, YAP, and LuAP) with respect to the ideal cuboctahedron (cf. Fig. 3 and Table II). In the case of LaAP the gap we are looking for was not yet formed. Calculated higher value in LuAP (1.0 eV) than those in YAP (0.9 eV) and GdAP (0.6 eV) corresponds to an experimental trend. Experimental values found from absorption peaks of Fig. 1 are about 0.9 eV for LuAP and 0.7 eV for YAP hosts. The value 0.58 eV for GdAP host was reported in Refs. 12, 14, and 30. Hence, there is relatively good agreement between experimental and calculated gaps. Larger discrepancy is manifested between calculated and experimental separations of juxtaposed peaks. However, such discrepancies could be expected since only a minimal Ce cluster (Ce with its nearest neighbors) was considered. Moreover, substitution of Ce for Gd, Y, or Lu ions in the perovskite lattice is likely to deform the closest environment of the central ion of the cluster with respect to the original due to different ionic radius of Ce.

Having shown that one of the former T_{2g} levels splits off and gets close to the former E_g levels, one may also address a question *which* of the T_{2g} levels is expected to go down. Schemes in Figs. 4 and 5, as well as Table II, show that in the case of GdAP and YAP the d_{yz} orbital goes down while in LuAP it is that of d_{xy}. The reason probably can be found again in the way of how the structure in question is deformed with respect to that of ideal cuboctahedron. Close inspection of the true coordinates of oxygens in discussed perovskite structures compared to coordinates of corresponding ideal cuboctahedron obtained by our optimization procedure shows the following. In the case of $GdAlO_3$ and $YAlO_3$ it appears that ideal cuboctahedron is deformed in such a way that oxygens 11 and 12 (referring to Fig. 2 and Table III) are those which are pulled furthest away from the central ion. They are pulled in the *yz* plane and the extra space might cause the reduction in the energy of the d_{yz} orbital with respect to the orbitals d_{xy} and d_{xz}. In contrast, for LuAP the largest pullaway from the central ion concerns oxygens 3 and 4 in the *xy* plane which consistently promotes the reduction in the energy of d_{xy} orbital.

IV. CONCLUSION

We pursued an issue of an assignment of absorption 4*f*-5*d* transitions of Ce^{3+} ion in various $RAlO_3$ (R=La, Gd, Y, and Lu) hosts where Ce ion substitutes for the lattice R cation. To better understand the Ce environment in various hosts, the 12-coordinated R complex in true perovskite structures was by an optimization procedure transformed to an ideal cuboctahedral arrangement showing in detail how the two different structures are related. The deformation of an ideal cuboctahedron when passing to the true perovskite structure increases as the R ion becomes smaller. Using two semiempirical approaches we calculated the energy scheme associated with the 4*f*-5*d* transitions of the Ce^{3+} ion. The main objective was to confront the calculated results with intuitive assignments, previously made by some authors. Unlike those intuitive suggestions, calculated energy scheme manifests that two of the three low-energy levels originate predominantly from the former E_g doublet of an ideal cuboctahedron while the third level splits off the former T_{2g} triplet. Two upper levels are predominantly formed by split levels of former T_{2g}. It is worth noting that due to cuboctahedron distortion some of the resulting energy levels manifest a considerable mixing of contributions from former E_g and T_{2g} levels.

TABLE III. Cartesian coordinates (x,y,z) of the central atom and oxygens (numbers refer to Fig. 2) in both ideal cuboctahedron and true structure of GdAP, YAP, and LuAP. Coordinates of corresponding ideal cuboctahedron are calculated by optimization procedure described in the text.

GdAP						
No.	Ideal cuboctahedron (x,y,z)			Real structure (x,y,z)		
0	0.0000	0.0000	0.0000	0.0000	0.0000	0.0000
1	1.8650	1.8646	0.0000	2.2904	1.8998	0.0000
2	1.8650	−1.8650	0.0000	1.7698	−2.3686	0.0000
3	−1.8650	1.8650	0.0000	−1.9786	1.3853	0.0000
4	−1.8650	−1.8650	0.0000	−1.4272	−1.8125	0.0000
5	1.8650	0.0000	1.8650	1.7178	−0.1794	1.5774
6	1.8650	0.0000	−1.8650	1.7178	−0.1794	1.5774
7	−1.8650	0.0000	1.8650	−1.4948	−0.1644	2.1469
8	−1.8650	0.0000	−1.8650	−1.4948	−0.1644	−2.1469
9	0.0000	1.8650	1.8650	0.1013	1.9549	1.5774
10	0.0000	1.8650	−1.8650	0.1013	1.9549	−1.5774
11	0.0000	−1.8650	1.8650	0.1217	−2.2986	2.1469
12	0.0000	−1.8650	−1.8650	0.1217	−2.2986	−2.1469

YAP						
No.	Ideal cuboctahedron (x,y,z)			Real structure (x,y,z)		
0	0.0000	0.0000	0.0000	0.0000	0.0000	0.0000
1	1.8556	1.8556	0.0000	2.3859	1.8111	0.0000
2	1.8556	−1.8556	0.0000	1.8177	−2.5262	0.0000
3	−1.8556	1.8556	0.0000	−1.9526	1.2522	0.0000
4	−1.8556	−1.8556	0.0000	−1.2868	−1.8537	0.0000
5	1.8556	0.0000	1.8556	1.6820	−0.2682	1.5199
6	1.8556	0.0000	−1.8556	1.6820	−0.2682	−1.5199
7	−1.8556	0.0000	1.8556	−1.3696	−0.2201	2.1710
8	−1.8556	0.0000	−1.8556	−1.3696	−0.2201	−2.1710
9	0.0000	1.8556	1.8556	0.1282	1.9516	1.5199
10	0.0000	1.8556	−1.8556	0.1282	1.9516	−1.5199
11	0.0000	−1.8556	1.8556	0.1843	−2.4398	2.1710
12	0.0000	−1.8556	−1.8556	0.1843	−2.4398	−2.1710

LuAP						
No.	Ideal cuboctahedron (x,y,z)			Real structure (x,y,z)		
0	0.0000	0.0000	0.0000	0.0000	0.0000	0.0000
1	1.8475	1.8475	0.0000	1.9347	1.4692	−0.1419
2	1.8475	−1.8475	0.0000	−2.5175	2.2006	−0.2202
3	−1.8475	1.8475	0.0000	−2.5175	−2.2006	−0.2202
4	−1.8475	−1.8475	0.0000	1.1433	0.0000	1.9533
5	1.8475	0.0000	1.8475	1.1433	0.0000	1.9533
6	1.8475	0.0000	−1.8475	1.7637	0.0000	−2.4521
7	−1.8475	0.0000	1.8475	−1.8659	0.0000	1.1743
8	−1.8475	0.0000	−1.8475	−2.6422	0.0000	−1.8356
9	0.0000	1.8475	1.8475	−0.2507	2.2006	1.3005
10	0.0000	1.8475	−1.8475	−0.3322	1.4692	−1.6626
11	0.0000	−1.8475	1.8475	−0.2507	−2.2006	1.3005
12	0.0000	−1.8475	−1.8475	−0.3322	−1.4692	−1.6626

ACKNOWLEDGMENTS

The authors acknowledge the financial support of the Czech Projects No. GA AV IAA100100810 and No. ME 903 and the institutional research Plan No. AVOZ10100521. Special thanks are due to Carlo Mealli and Andrea Ienco for useful suggestions and discussion as well as to Mariya Zhuravleva and Tadeusz Lukasiewicz for providing the samples of YAP:Ce and LuAP:Ce, respectively, for absorption measurements.

[1] H. R. Lewis, J. Appl. Phys. **37**, 739 (1966).
[2] C. D. Brandle, J. Cryst. Growth **264**, 593 (2004).
[3] M. J. Weber, Solid State Commun. **12**, 741 (1973).
[4] R. Autrata, P. Schauer, Jos. Kvapil, and J. Kvapil, J. Phys. E **11**, 707 (1978).
[5] M. J. Weber, J. Appl. Phys. **44**, 3205 (1973).
[6] T. Takeda, T. Miyata, F. Muramatsu, and T. Tomiki, J. Electrochem. Soc. **127**, 438 (1980).
[7] E. Autrata, P. Schauer, J. Kvapil, and Jos. Kvapil, Scanning **5**, 91 (1983).
[8] M. Nikl, Phys. Status Solidi A **178**, 595 (2000).
[9] T. Hoshina and S. Kuboniwa, J. Phys. Soc. Jpn. **31**, 828 (1971).
[10] D. J. Robbins, J. Electrochem. Soc. **126**, 1550 (1979).
[11] P. A. Tanner, L. Fu, L. Ning, B.-M. Cheng, and M. G. Brik, J. Phys.: Condens. Matter **19**, 216213 (2007).
[12] P. Dorenbos, J. Lumin. **99**, 283 (2002).
[13] T. Tomiki, H. Ishikawa, T. Tashiro, M. Katsuren, A. Yonesu, T. Hotta, T. Yabiku, M. Akamine, T. Futemma, T. Nakaoka, and I. Miyazato, J. Phys. Soc. Jpn. **64**, 4442 (1995).
[14] J. W. M. Verweij, M. Th. Cohen-Adad, D. Bouttet, H. Lautesse, B. Moine, and C. Pedrini, Chem. Phys. Lett. **239**, 51 (1995).
[15] A. J. Wojtowicz and S. Janus, *Book of Abstracts*, IEEE Ninth International Conference on Inorganic Scintillators and their Applications (SCINT2007) (Wake Forest University, NC, USA, 2007), p. 132.
[16] S. Kammoun and M. Kamoun, Phys. Status Solidi B **229**, 1321 (2002).
[17] M. Johnsson and P. Lemmens, J. Phys.: Condens. Matter **20**, 264001 (2008).
[18] J. S. Zhou and J. B. Goodenough, Phys. Rev. B **77**, 132104 (2008).
[19] A. Vedda, M. Fasoli, M. Nikl, V. V. Lagute, E. Mihokova, J. Pejchal, A. Yoshikawa, and M. Zhuravleva (unpublished).
[20] W. Drozdowski, A. J. Wojtowicz, T. Lukasiewicz, and J. Kisielewski, Nucl. Instrum. Methods Phys. Res. A **562**, 254 (2006).
[21] M. A. Arillo, J. Gomez, M. L. Lopez, C. Pico, and M. L. Veiga, J. Mater. Chem. **7**, 801 (1997).
[22] M. Wolfsberg and L. J. Helmholz, J. Chem. Phys. **20**, 837 (1952).
[23] C. E. Schäffer and C. K. Jørgensen, Mol. Phys. **9**, 401 (1965).
[24] M. Bacci, Jpn. J. Appl. Phys., Part 2 **27**, L1699 (1988).
[25] M. Bacci, New J. Chem. **17**, 67 (1993).
[26] C. Mealli and D. Proserpio, J. Chem. Educ. **67**, 399 (1990).
[27] R. Hoffmann and W. N. Lipscomb, J. Chem. Phys. **36**, 2179 (1962); **37**, 2872 (1962).
[28] G. Blasse and A. Brill, J. Chem. Phys. **47**, 5139 (1967).
[29] E. van der Kolk, J. T. M. de Haas, A. J. J. Bos, C. W. E. van Eijk, and P. Dorenbos, J. Appl. Phys. **101**, 083703 (2007).
[30] J. A. Mares, C. Pedrini, B. Moine, K. Blazek, and J. Kvapil, Chem. Phys. Lett. **206**, 9 (1993).
[31] H. Lehnert, H. Boysen, P. Dreier, and Y. Yu, Z. Kristallogr. **215**, 145 (2000).
[32] D. du Boulay, N. Ishizawa, and E. N. Maslen, Acta Crystallogr., Sect. C: Cryst. Struct. Commun. **60**, i120 (2004).
[33] N. L. Ross, J. Zhao, and R. J. Angel, J. Solid State Chem. **177**, 1276 (2004).